High speed imaging of micro-sized droplet jetted on surface with wettability pattern

Lim, Chun Yee; Lam, Yee Cheong

2014

Lim, C. Y. and Lam, Y. C. (2014). High Speed Imaging of Micro-sized Droplet Jetted on Surface with Wettability Pattern. The 9th International Conference on MicroManufacturing (no. 77).

https://hdl.handle.net/10356/102901

High Speed Imaging of Micro-sized Droplet Jetted on Surface with Wettability Pattern

ICOMM 2014 No. 77

Lim Chun Yee[1], Lam Yee Cheong[1]

[1] *NanyangTechnological University, School of Mechanical and Aerospace Engineering, Singapore*

Abstract

Experimental results based on high speed imaging of micro-sized droplet jetted on a hydrophobic surface with hydrophilic lines are presented. The effects of the hydrophilic line and the initial impact offset distance from the line on the droplet spreading behaviour are studied. Two distinct processes have been identified, namely the centering and conforming processes. During the centering process, the droplets which impinge at a certain offset distance from the center of the hydrophilic lines migrate towards the center of the line. A droplet with a larger offset distance experiences a slower centering process. This conforming process involves droplets elongate along the hydrophilic line, causing the droplet to conform to the wettability pattern. The outcome of this study can be applied to inkjet printing process for the enhancement of material deposition accuracy and tolerance of printed micro-sized features.

Keywords: Inkjet printing, wettability contrast, surface modification.

1. Introduction

1.1. Background

Inkjet printing technology has been applied to various applications beyond its original purpose of printing text or images on papers. Metals [1], ceramics [2] and polymers [3] can be deposited directly on a solid substrate through inkjet printing technology. It has potential applications in manufacturing of plastic transistor circuits [4], light emitting diode (LED) display [5] and formation of thin films [6].

The diameter of an inkjet droplet that can be generated from a typical inkjet dispenser ranges from 10 to 100μm [7]. This set a limit to the resolution of the printed features. Surface wettability patterning has been proposed to overcome this limit and to achieve features which are smaller than the droplet size. Upon impingement, inkjet droplet is steered away from the hydrophobic area and guided to spread along the hydrophilic pattern to form the desired feature.

1.2. Literature review

Despite its significance, the dynamics of droplet impingement on a non-homogenous surface is seldom studied in the literature. Leopoldes et al [8] experimentally studied the final droplet shape of a micro-sized droplet after it was jetted on a chemically heterogeneous surface. Typically, the end results of the printing process were studied instead of the dynamic process. This is partially due to the difficulties in capturing the impact process of micro-sized droplet which occurs in a very short time scale. Millimetre-size droplet spreading process on a heterogeneous surface which occurs over a longer time scale has been investigated in the literature [9].

Recent advances in high speed imaging have permitted the observations of the spreading dynamics of micro-sized droplets. Eddi et al [10] captured the short time dynamics during the spreading process of water-glycerine droplet attached to a needle and deposited on a glass

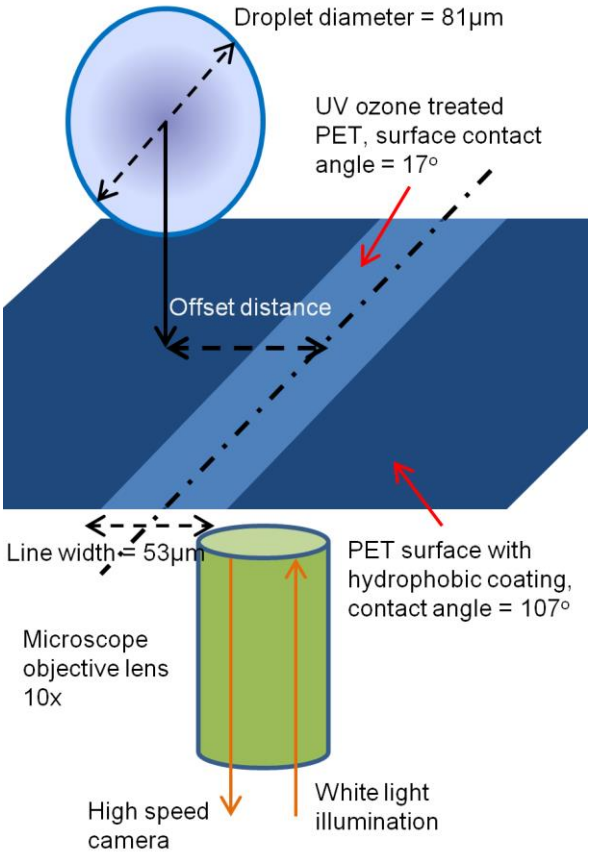

Fig. 1. Experimental setup for high speed imaging of micro-sized droplet impinging and spreading on hydrophilic line.

substrate, with a capturing rate as high as 250,000 frame per second (fps). Briones et al [11] studied the impact and spreading of a micro-sized water droplet on an aluminum thin film at a maximum frame rate of 120,000 fps. Brown et al [12] investigated the effect of surface roughness on the impact and spreading of a picoliter water droplet, with a frame rate of 90,000 fps. However, their investigation focused on the spreading dynamics of droplet on a homogenous surface without any wettability patterns.

This paper presents the high speed imaging and experimental analysis of a micro-sized droplet jetted on a surface with wettability patterns. Specifically, the experimental investigation aims to reveal the interaction between the impinging droplet with the hydrophilic line across a hydrophobic surface. A proper understanding of this process can improve the accuracy of material deposition and allow smaller features to be printed on a substrate.

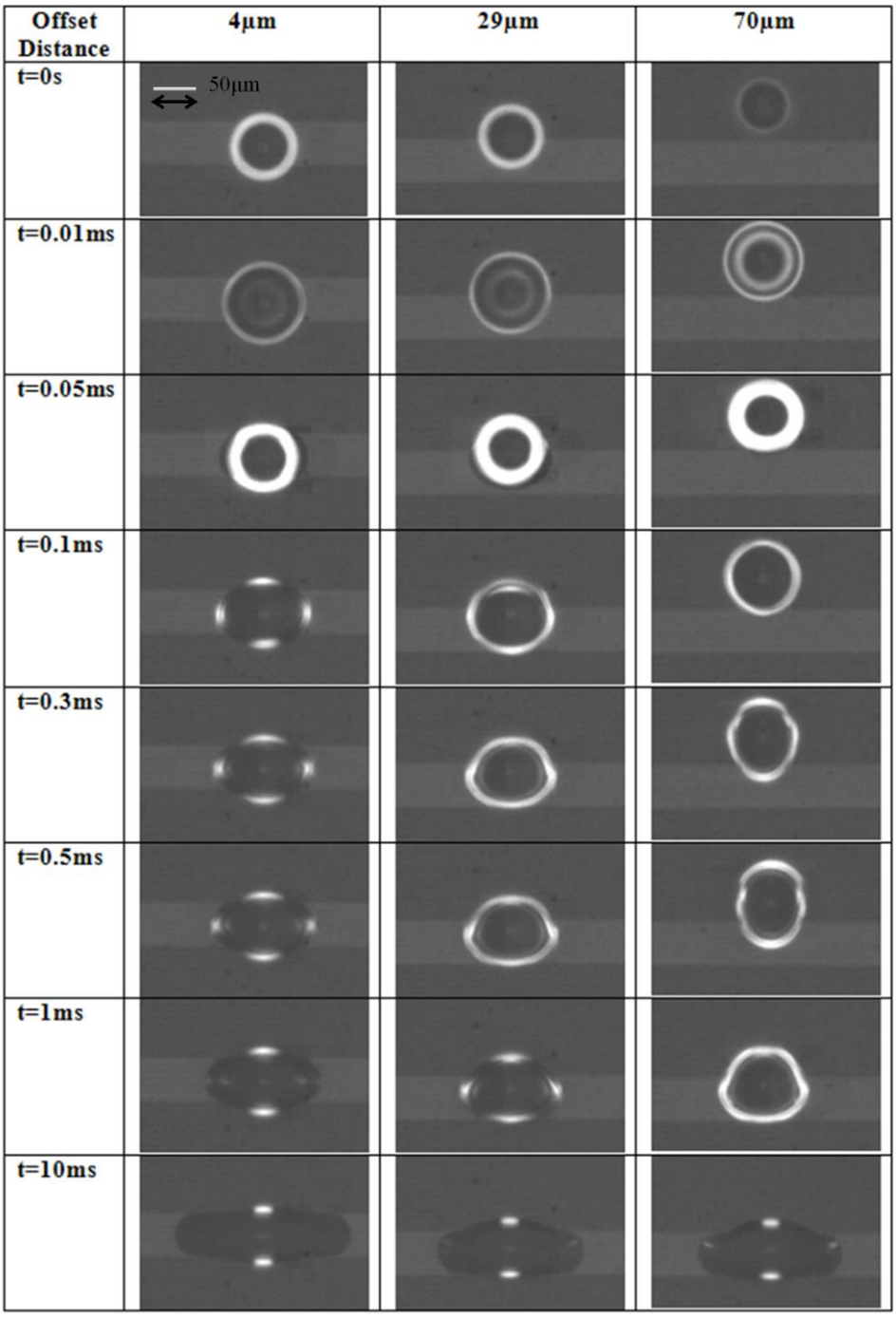

Fig. 2. Bottom view of droplet impingement and spreading on hydrophilic line on PET surface.

2. Experimental Setup

2.1. Surface patterning

The substrate employed in the experiments is polyethylene terephthalate (PET) sheet, which is a common material for roll-to-roll manufacturing process. The surface of the PET sheet was first dip-coated with 3M Novec 1700 electronic grade coating which is a clear solution with fluorochemical acrylic polymer carried in a hydrofluoroether solvent. The concentration of the solution is diluted to 0.1 weight % from the original concentration of 2% to reduce the coating thickness and time for selective removal of coating. Immediately after coating, the solvent is evaporated in an oven at 120°C for 10 seconds. The coating increases the contact angle of the PET sheet, rendering it hydrophobic.

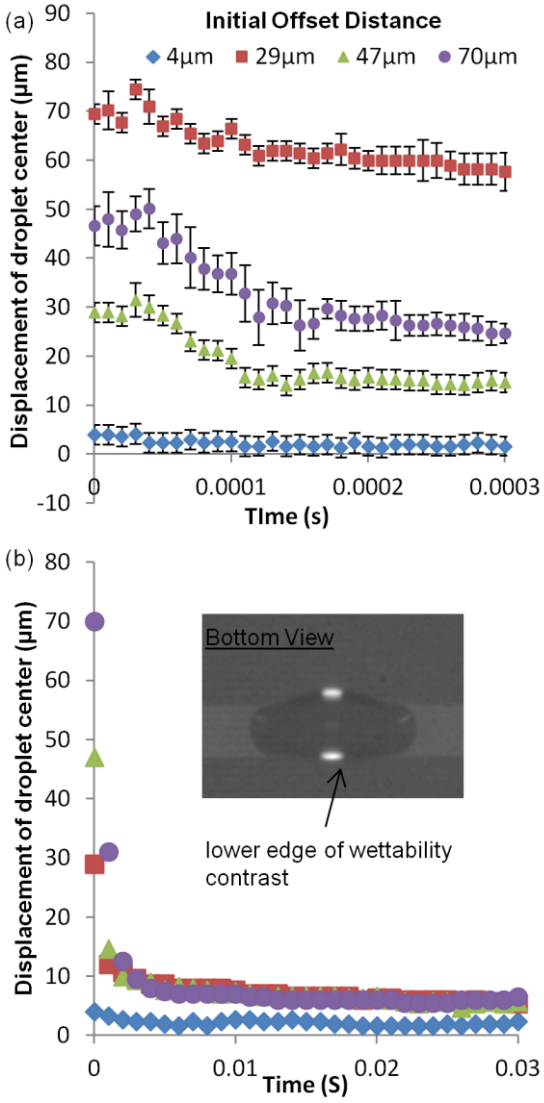

Fig. 3. Displacement of droplet center from center of hydrophilic line at different initial offset distances (a) for short time scale (b) for longer time scale. Inset shows that the lower edge of the wettability contrast impeded the completeness of centering process. Error bar is not shown in (b) for clarity.

To create hydrophilic patterns on the PET sheet, a nickel mask of 50µm thick with long slits was placed on top the coated PET sheet. Magnet was placed below the PET sheet to hold the nickel mask firmly against the PET surface. The sandwich was then placed into ultra-violet (UV) ozone exposure unit (Senlight PL16) which generates 10.2 mW/cm^2 of UV with 185nm wavelength and 32.7 mW/cm^2 of UV with 254nm wavelength for 25 minutes. The treatment selectively removed the hydrophobic coating according to the slits on the mask. It modified the exposed area on the PET sheet into hydrophilic region.

The fidelity of the patterning process through UV exposure with the nickel mask was inspected. The average width of the slits on the nickel mask was measured to be 48µm. The average width of the hydrophilic lines of the PET surface was measured to be 53µm, which is approximately 10% larger than the slits. The accuracy of the patterning process can be potentially improved by employing a vacuum suction system instead of magnets to hold the mask against the PET surface.

The average contact angles of the hydrophobic coated and UV ozone modified PET surfaces were measured to be 107° and 17° respectively. This process produced hydrophilic lines of with a high wettability contrast of 90° to the surrounding hydrophobic surface.

2.2. Droplet dispensing and high speed imaging

Water droplet was jetted on the surface with an inkjet dispenser head (MD-K-130 Microdrop Technologies) with a nozzle diameter of 70µm. A driving voltage pulse of 105V with 30µs pulse width generated a droplet of 81µm in diameter. The droplet impinged the PET substrate with various offset distances from the hydrophilic lines.

The experimental setup is shown in Fig. 1. The bottom view of the droplet impingement and spreading process was captured through a high speed camera (Photron Fastcam SA5 monochrome) attached to an inverted microscope (Nikon Ti-S Eclipse). The capturing rate of the camera was set to 100,000 fps. Due to the short exposure time, a high intensity light source was required to capture the images at high speed. The white light illumination was supplied by ultra high pressure mercury lamp (Nikon Intensilight 130W). A UV cut-off filter was attached to the filter cube of the microscope to remove the UV component from the light source.

3. Experimental Result and Discussion

Fig. 2 shows the bottom view of droplets impinging and spreading at different offset distances relative to the center of a hydrophilic line. All droplets spread and elongated along a hydrophilic line due to the high wettability contrast between the line and the surrounding surface. The evolution of a droplet can be divided into two distinct processes, namely the centering process and the conforming process.

3.1. Centering process

Droplets which were not impinged exactly at the centre of the hydrophilic line moved or migrated towards the centre of the line. This movement was driven by the difference in surface energy for hydrophobic and hydrophilic regions. Fig. 3 shows the displacement of the droplet center from the center of the hydrophilic lines at various initial offset distances. Each data point in Fig. 3 represents an average of 2 to 3 experimental runs, with approximately similar initial offset distances. The stated offset distance is an average of these runs.

Droplets with 4µm offset showed little migration since they

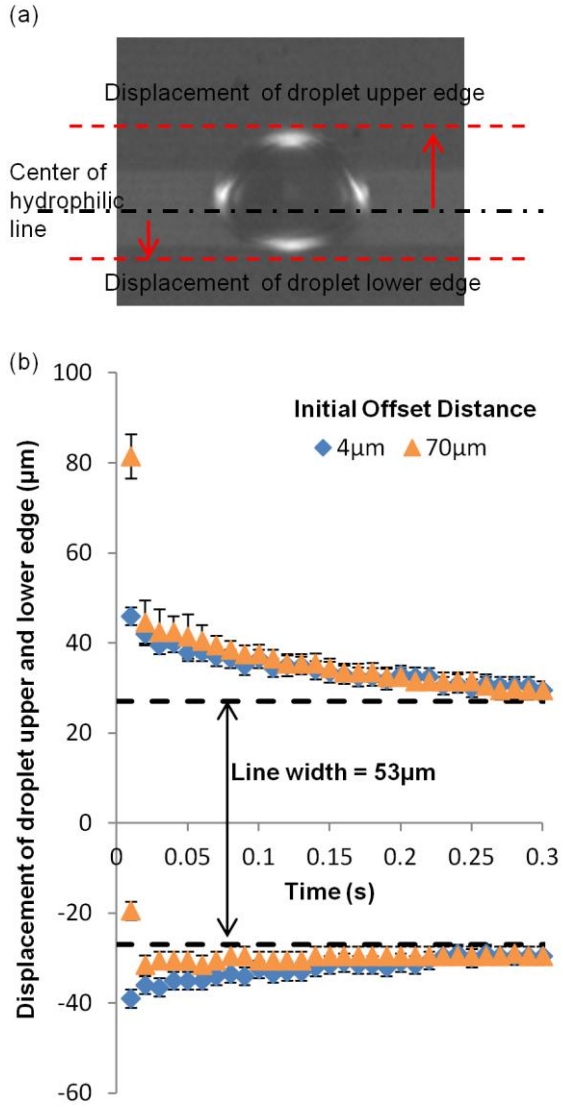

Fig. 4 (a) Definition for displacement of upper and lower edges of droplet relative to center of hydrophilic strip. (b) Time evolution of upper and lower edges of droplet relative to hydrophilic line.

were deposited at close proximity to the center of the line. Droplets deposited 29μm and 47μm from the center of the line exhibited a quick migration process towards the center of the line during the first 100μs after impingement. Droplets deposited much further away (70μm) showed a much slower centering process.

This could be attributed to the difference in initial contact surface of droplet upon impingement. For a droplet deposited at 29μm from the center, approximately half of the droplet base was in contact with the hydrophilic area (see Fig. 2). On the contrary, for a droplet deposited with 70μm offset, only a small portion of the droplet base touched the hydrophilic area initially.

Fig 3(b) shows the displacement of droplet center in a longer time frame, up to 30ms. Residual offset of 5 to 7μm persisted for all droplets except for the droplet with initial offset of 4μm. The migration of droplet towards the center was impeded by the lower edge of wettability contrast, as shown in Fig 2 and the inset of Fig 3(b).

3.2. Conforming process

Besides inducing the migration of the droplet towards the center of the line, the hydrophilic region also elongated the droplet to conform to the edges of the wettability pattern. Typically, after the centering process, part of the droplet would still lie outside of the hydrophilic region, especially when the line width was smaller than the droplet base diameter.

When a droplet spread along the direction of the hydrophilic line, liquid from the center was directed away to the left and right of the line (see Fig 2). As a result of mass continuity, the upper and lower edges of the droplet were pulled into the hydrophilic region and conformed to the wettability contrast. The conforming process was approximately two orders of magnitude slower than the centering process and it was completed after 0.3 seconds from impingement. The conforming process was not affected by the initial offset distance, as shown in Fig. 4. The displacements of the upper and lower edges of droplet impinging with 4μm and 70μm offset were almost identical, except only for the early stage during the centering process.

This behaviour is important for the manufacturing process with inkjet printing. The final printed feature is independent on the initial impact location provided that part of the droplet touches the hydrophilic line. It will then migrate towards the line and conform to its line width. This behaviour enhances the robustness of the inkjet printing process, with accurate final droplet deposition and good control over the printed line width.

3.3. Theoretical analysis

Theoretical analysis on droplet migration process on a surface with a linear wettability gradient has been performed by Subramanian et al [13]. The formulation for droplet migration velocity across a linear wettability gradient is not expected to describe droplet movement accurately on a surface with sharp wettability contrast because the latter involves significant droplet distortion and elongation while the former assumes a spherical cap. However, a theoretical analysis on the initial driving force induced by the wettability contrast to initiate the migration of the droplet towards the hydrophilic region will be helpful to provide an insight on the experimental results. The analysis by Subramanian et al is adapted here for the current investigation of droplet movement induced by a sharp wettability constrast.

For a droplet which is impinged at a finite offset from the center of the hydrophilic line, the net driving force towards the hydrophilic area F is induced by difference in interfacial forces on opposite edges of the droplet (see Fig. 5). With Young's equation, F can be obtained by integrating the interfacial force difference (along the direction perpendicular to the hydrophilic line) around the circumference of the droplet footprint:

$$F = 2R\sigma \int_0^{\pi/2} [\cos\theta_f - \cos\theta_r] \cos\phi d\phi \qquad (1)$$

where R is the radius of droplet circular base/footprint, σ is the surface tension, ϕ is the polar angle, θ_f and θ_r are the contact angles in the front and rear edge of the droplet respectively as depicted in Fig. 5. Due to symmetry, the integration can be performed from 0 to π/2, with a factor of two added to the integration (see Eq. 1). Let the distance from the center of the droplet to the edge of the hydrophilic line be d. The integration in Eq. 2 can be separated into two parts,

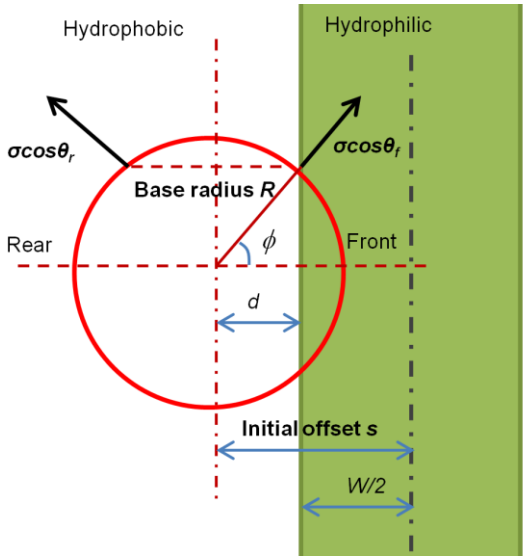

Fig. 5 Plan view of droplet which straddles across sharp wettability contrast

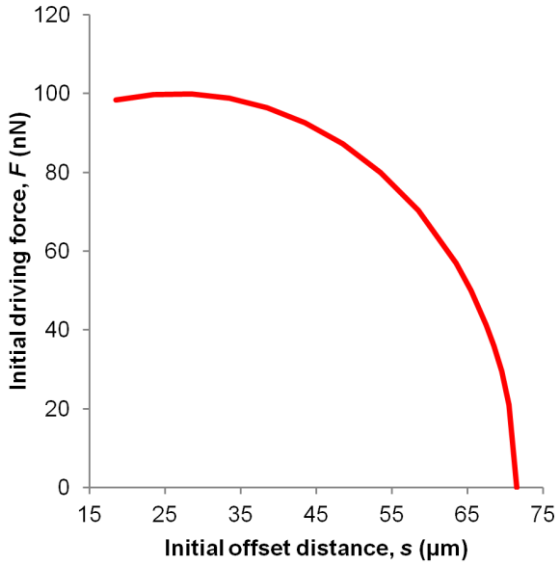

Fig. 6 Theoretical driving force on droplet induced by wettability contrast at various offset distances. Hydrophilic line width W = 53μm. Droplet base radius R = 45μm

$$F = 2R\sigma\left[\int_0^{\cos^{-1}(d/R)}(\cos\theta_f - \cos\theta_r)\cos\phi d\phi + \int_{\cos^{-1}(d/R)}^{\pi/2}(\cos\theta_f - \cos\theta_r)\cos\phi d\phi\right] \quad (2)$$

The second term on the right hand side of Eq. 2 is zero because the front and rear contact angles are the same (θ_f = θ_r) in that region. The integration in Eq. 3 can thus be performed and simplified as,

$$F = 2R\sigma(\cos\theta_A - \cos\theta_B)\sin\left[\cos^{-1}(d/R)\right] \quad (3)$$

where θ_A and θ_B are the contact angles of the hydrophilic and hydrophobic surfaces respectively. By relating d to the initial offset distance, s and the width of the hydrophilic line W, Eq 3 can be written as

$$F = 2\sigma(\cos\theta_A - \cos\theta_B)\sqrt{R^2 - (s - W/2)^2} \quad (4)$$

Based on the experimental images, the initial radius of droplet footprint R is determined to be 45μm. The driving force F is plotted against the initial offset distance in Fig 5. As the initial offset distance s increases, F decreases according to Eq. 4 because only a small sector on the droplet experiences the interfacial force difference. This explains the slower centering process for a droplet at a larger offset distance from the hydrophilic line, as demonstrated in our experimental results in Fig. 3

Eq. 4 is only valid when s is smaller than R+W/2, which is the upper limit of offset distance for droplet movement towards the hydrophilic line. If the offset distance is larger than the upper limit, the droplet is not in contact with the hydrophilic line at all. The lower limit of offset distance for Eq. 5 to be valid is R-W/2 where the front edge of the droplet coincides with the other edge of the hydrophilic line.

4. Conclusions

The bottom view images of a jetted droplet on a hydrophilic line over a hydrophobic surface have been captured through a high speed camera. The effects of the hydrophilic line on the droplet movement and spreading behavior have been studied. Two distinct processes have been identified, namely centering process and conforming process. During the centering process, a droplet which is impinged at a finite offset distance from the center of the hydrophilic lines migrates towards the center of the line. This process which happens at a time scale below 1ms is dependent on the initial offset distance. A droplet with a larger offset distance experiences a slower centering process.

A droplet with a base diameter larger than the line width cannot fit completely into the patterned line after the initial centering process. The conforming process involves droplets elongated along the hydrophilic line, causing the upper and lower edges of the droplet to conform to the wettability pattern. This process is completed after approximately 0.3sec, regardless of the initial offset distance.

A theoretical analysis has been performed to determine the driving force on the droplet due to the wettability contrast which induces droplet migration toward the hydrophilic region. The analysis shows that the driving force decreases with increasing initial offset distance. This agrees with the experimental results which demonstrate a slower migration at a larger initial offset distance.

This study reveals the interaction of micro-sized droplet with hydrophilic patterns and shows that wettability patterning can potentially enhance the robustness for producing micro-sized features with inkjet printing.

Acknowledgements

The authors gratefully acknowledge the Agency for Science, Technology and Research (A*STAR) Singapore for its financial support (grant no. 102 170 0140).

References

[1] S. Gamerith, et al., Direct Ink-Jet Printing of Ag–Cu Nanoparticle and Ag-Precursor Based Electrodes for OFET Applications. Adv. Funct. Mater., 2007. **17**(16): p. 3111-3118.

[2] T. Wang, et al., Ink-Jet Printing and Sintering of PZT. J. Am. Ceram. Soc., 2005. **88**(8): p. 2053-2058.

[3] H.Y. Gan, et al., Reduction of droplet volume by controlling actuating waveforms in inkjet printing for micro-pattern formation. J. Micromech. Microeng., 2009. **19**(5): p. 055010.

[4] H. Sirringhaus, et al., High-Resolution Inkjet Printing of All-Polymer Transistor Circuits. Science, 2000. **290**(5499): p. 2123-2126.

[5] H.S. Koo, et al., Fabrication and chromatic characteristics of the greenish LCD colour-filter layer with nano-particle ink using inkjet printing technique. Displays, 2006. **27**(3): p. 124-129.

[6] C.-T. Chen, et al., Dynamic evolvement and formation of refractive microlenses self-assembled from evaporative polyurethane droplets. Sens. Actuators, A, 2008. **147**(2): p. 369-377.

[7] M.I. Hutchings, et al., Inkjet Technology for Digital Fabrication. 2013: John Wiley & Sons Ltd. p. 1.

[8] J. Léopoldès, et al., Jetting Micron-Scale Droplets onto Chemically Heterogeneous Surfaces. Langmuir, 2003. **19**(23): p. 9818-9822.

[9] O. Bliznyuk, et al., Directional Liquid Spreading over Chemically Defined Radial Wettability Gradients. ACS Appl. Mater. Interfaces, 2012. **4**(8): p. 4141-4148.

[10] A. Eddi, et al., Short time dynamics of viscous drop spreading. Phys. Fluids, 2013. **25**(1): p. 013102.

[11] A.M. Briones, et al., Micrometer-Sized Water Droplet Impingement Dynamics and Evaporation on a Flat Dry Surface. Langmuir, 2010. **26**(16): p. 13272-13286.

[12] P.S. Brown, et al., Impact of Picoliter Droplets on Superhydrophobic Surfaces with Ultralow Spreading Ratios. Langmuir, 2011. **27**(22): p. 13897-13903.

[13] R.S. Subramanian, et al., Motion of a Drop on a Solid Surface Due to a Wettability Gradient. Langmuir, 2005. **21**(25): p. 11844-11849.